OXFORD

Cerebral Cortex, 2023, **33**, 8179–8193
https://doi.org/10.1093/cercor/bhad107
Advance access publication date 25 March 2023
Original Article

Interhemispheric differences of pyramidal cells in the primary motor cortices of schizophrenia patients investigated postmortem

Péter Szocsics[1,2], Péter Papp[3], László Havas[4,5], János Lőke[5], Zsófia Maglóczky[1,*]

[1]Human Brain Research Laboratory, Institute of Experimental Medicine, ELKH, Budapest 1083, Hungary,
[2]János Szentágothai Doctoral School of Neuroscience, Semmelweis University, Budapest 1085, Hungary,
[3]Cerebral Cortex Research Group, Institute of Experimental Medicine, ELKH, Budapest 1083, Hungary,
[4]Department of Pathology, Szt. Borbála Hospital, Tatabánya 2800, Hungary,
[5]Department of Psychiatry, Szt. Borbála Hospital, Tatabánya 2800, Hungary

*Corresponding author: Zsófia Maglóczky, Institute of Experimental Medicine, ELKH, Szigony u. 43., Budapest 1083, Hungary. Email: magloczky.zsofia@koki.hu

Motor disturbances are observed in schizophrenia patients, but the neuroanatomical background is unknown. Our aim was to investigate the pyramidal cells of the primary motor cortex (BA 4) in both hemispheres of postmortem control and schizophrenia subjects—8 subjects in each group—with 2.5–5.5 h postmortem interval. The density and size of the Sternberger monoclonal incorporated antibody 32 (SMI32)-immunostained pyramidal cells in layer 3 and 5 showed no change; however, the proportion of larger pyramidal cells is decreased in layer 5. Giant pyramidal neurons (Betz cells) were investigated distinctively with SMI32- and parvalbumin (PV) immunostainings. In the right hemisphere of schizophrenia subjects, the density of Betz cells was decreased and their PV-immunopositive perisomatic input showed impairment. Part of the Betz cells contained PV in both groups, but the proportion of PV-positive cells has declined with age. The rat model of antipsychotic treatment with haloperidol and olanzapine showed no differences in size and density of SMI32-immunopositive pyramidal cells. Our results suggest that motor impairment of schizophrenia patients may have a morphological basis involving the Betz cells in the right hemisphere. These alterations can have neurodevelopmental and neurodegenerative explanations, but antipsychotic treatment does not explain them.

Key words: antipsychotics; human brain; immunohistochemistry; neuropathology; parvalbumin.

Introduction

Schizophrenia is a psychiatric disorder with a mean lifetime morbid risk of ~7.2 per 1,000 people (McGrath et al. 2008).The first episode of the disease typically begins in young adulthood, often with hallucinations, delusions, or bizarre behavior—the so-called positive symptoms (Boland and Verduin 2021). Schizophrenia affects a broad range of other mental functions as well, such as mood, motivation, social functioning, thoughts, or cognition. Some of these disturbances appear before the first psychotic episode and recent theories suggest that the impaired function of perception and cognition could explain the development of later positive symptoms (Friston et al. 2016).

In addition, an increasing number of studies suggest that motor functions are also impaired in patients with schizophrenia (Walther and Strik 2012; Walther 2015). The use of antipsychotics—the first-line medications of the disorder—could also affect movements through the nigrostriatal pathway and cause drug-induced Parkinsonism (Ward and Citrome 2018). It is important to mention that the initial descriptions of schizophrenia also listed a wide range of disturbances of motor function, mostly categorizing them as catatonic symptoms (Kraepelin 1919; Bleuler 1950) such as stupor, mutism, and automatic obedience. Further motor disturbances were described, such as hypokinesia, involuntary movements, and dystonia, considered to belong to the extrapyramidal symptoms (EPSs), and are detectable in drug-naïve patients as well (Peralta et al. 2010). One interesting example of the presentation of motor symptoms was the study which compared childhood home videos of schizophrenia patients, their siblings, and not-related control population (Walker et al. 1994). It revealed that before the age of two significantly more motor symptoms appear in the people who are later affected by the disorder, especially on the left (subdominant) side of the body. Other studies imply that the investigation of motor symptoms could lead to a better understanding of the neurodevelopmental nature of schizophrenia (Filatova et al. 2017; Hirjak et al. 2018).

From the 19th century until today, several attempts have been made to explain the development of schizophrenia by structural changes in the brain, but in many cases, the neuropathological results were inconsistent and contradictory (Harrison 1999). The most common findings among volume-based studies are the decrease in cortical gray matter and an enlargement of ventricular volume (Glahn et al. 2008). Furthermore, damages of fibers in the white matter have also been described, suggesting that disconnection between different brain areas might explain the

Received: June 1, 2022. **Revised:** March 2, 2023. **Accepted:** March 3, 2023

symptoms of schizophrenia (Schneiderman et al. 2011). Decreases in pyramidal cell density have also been described in several neocortical areas (Benes et al. 1986), but no signs of neurodegeneration have typically been observed. Several studies have found the dysfunction of interneurons (Hashimoto et al. 2008; Kaar et al. 2019), primarily parvalbumin (PV) containing cells, which also affects pyramidal cell function (Lewis et al. 2012). If the two hemispheres of the human brain were studied distinctively, the asymmetry between them was typically reduced in schizophrenia patients (Cullen et al. 2006). However, there are some studies that describe the vulnerability of the subdominant side (Walker et al. 1994; Hashimoto et al. 2008; Hidese et al. 2018). One possible explanation for inconsistent results might be that the disease lead to the disturbance of the fine structure known to be strongly affected by the postmortem interval (PMI; Glausier et al. 2019).

Our research group has the opportunity to examine well-preserved human brain tissue with short, 2.5–5.5 h PMI. The cortical region of interest (ROI) in this study is the primary motor cortex (Brodmann's area 4—BA 4) and its differences between control subjects and patients with schizophrenia. The area plays a central role in motor control; however, its exact role is not fully understood yet (Omrani et al. 2017). Furthermore, BA 4 is connected to a wide range of brain areas such as the parietal and prefrontal neocortical regions, the basal ganglia, cerebellum, and the ventrolateral nucleus of thalamus (Dum and Strick 2002). The most striking cell type of BA 4 is the giant pyramidal cell or Betz cell (Betz 1874). A huge number of pyramidal cells of BA 4 form corticospinal connections (Groos et al. 1978). The number of cortico-motoneuronal connections shows positive correlation with the ability of fine motor movements (Lemon 2008), which appears to be impaired in psychotic disturbances (Carey et al. 2019). According to our previous study, the majority of Betz cells' somata express PV (Szocsics et al. 2021).

All of the Betz cells show immunoreactivity against Sternberger monoclonal incorporated antibody 32 (SMI-32) (Tsang et al. 2000; Szocsics et al. 2021), which labels the nonphosphorylated form of neurofilament H in humans and rats and neurofilament M in human samples (Lee et al. 1988). A subset of neocortical pyramidal cells are labeled in both species, a higher proportion in humans (Hayes and Lewis 1992) than in rats (Kirkcaldie et al. 2002), and show different distribution across cortical regions. SMI-32-immunoreactive pyramidal cells are present in layer 3, 5, and 6 in the human primary motor cortex (Hayes and Lewis 1992). SMI-32-immunreactivity is present in high number among longer, associative cortico-cortical projecting neurons and lesser in callosal or limbic projecting pyramidal cells (Hof et al. 1995). Naturally, cortico-subcortical projecting neurons can also express SMI-32. Functionally, these neurofilaments are considered to play a role in axonal and dendritic transport and morphology (Campbell and Morrison 1989).

Our aim in this study was to examine Betz- and other SMI32-immunopositive pyramidal cells of BA 4 and their PV-containing perisomatic input, since impairment of the somatic input has been described in previous studies of the prefrontal areas (Lewis et al. 2012). We particularly focused on examining the 2 hemispheres separately and comparing them. Additionally, we used an animal model of antipsychotic treatment (Lipska et al. 2003) to determine whether medication could lead to changes in the SMI32-immunoreactive pyramidal cells of the primary motor cortex.

Our hypothesis is that motor disturbances found in schizophrenia indicate neuronal changes in the primary motor cortex and pyramidal cells, especially Betz cells would be affected by the disorder.

Materials and methods

Human samples

Tissue blocks from the precentral gyri were dissected from the brains of 8 control (CTR) and 8 schizophrenia (SZ) subjects (with identification SKO# and SKIZ#, respectively). In 6 CTR and 6 SZ cases both hemispheres, and in 2–2 cases, only right hemispheres were sampled. All procedures were approved by the Regional Committee of Science and Research Ethics of Scientific Council of Health (ETT TUKEB 31443/2011/EKU, renewed: ETT TUKEB 15032/2019/EKU) and carried out in compliance with the Declaration of Helsinki. Autopsy of the subjects and collection of clinical data were made by the clinicians in the Pathology and Psychiatry Departments of St. Borbála Hospital, Tatabánya. Written informed consent for the study was obtained from the next of kin of the patients. Control subjects had no history of psychiatric or neurologic deficits, and their deaths were not caused directly by any brain damage. Schizophrenia patients were diagnosed by ICD-10 criteria (F20.x diagnoses) and meet the same exclusion criteria as the control subjects, except for the diagnosis of the disorder. The relevant features of the samples such as age, gender, PMI, or examined hemispheres are listed in Table 1. We checked whether any significant difference in age or PMI occurred between control and schizophrenia subjects.

The brains were perfusion fixed with Zamboni solution containing 4% paraformaldehyde, 0.00 or 0.05% glutaraldehyde, and 0.2% picric acid in 0.1 M phosphate buffer (PB, pH = 7.4, 2-h long 4 L). After perfusion, blocks from the precentral gyrus, which contain the primary motor cortical region—BA 4 (Brodmann 1909), were removed from the upper region of the lateral surface, representing the upper limb region (Penfield and Boldrey 1937). Sampling of blocks and determination of BA 4 was detailed in our previous article (Szocsics et al. 2021). Briefly, ∼0.5- to 1-cm-thick tissue blocks from the lateral part of the precentral gyrus were removed for the analysis. The blocks were postfixed in Zamboni solution, but without glutaraldehyde at 4 °C. Next day, the blocks were rinsed in 0.1 M PB solution 4 × 20 min and stored in 30% sucrose solution of 0.1 M PB after that at 4 °C for 2 days. Afterward, blocks were frozen over liquid nitrogen and stored at −80 °C. One sample (SKIZ4) was not perfused. In that case, tissue blocks were removed from an unfixed brain and placed and rinsed in Zamboni solution until the next day.

Immunohistochemistry

In case of use, the blocks were cut to 60-μm sections with a vibratome. The sections were washed four times in 0.1 M PB and stored in 30% sucrose solution of 0.1 M PB for 1 or 2 days at 4 °C. Next day, the sections were freeze-thawed 3 times over liquid nitrogen and washed in 0.1 M PB again. Endogenous peroxidase activity was blocked with 1% H_2O_2 solution of TRIS-buffered saline (TBS) for 10 min. After 10 min of TBS, washing nonspecific immunoglobulin-binding with 2% normal horse serum or normal goat serum or bovine serum albumin was blocked for 45 min. In case of fluorescent immunohistochemistry, additional 0.1% Triton-X was administered to the blocking solution, to increase membrane permeability and the signal of antibodies.

After washing with TBS, the following antisera were used for two days at 4 °C: anti-SMI32 (Biolegend, mouse 1:4,000, for 3,3′-diaminobenzidine-tetrahydrochloride—DAB and fluorescent immunohistochemistry), which labels the nonphosphorylated

Table 1. General data of subjects.

Subject code	Gender	Age (years)	PMI (hh:mm)	Cause of death (ICD-10 diag.)	Hemisphere(s) investigated
SKO2	male	74	04:55	Bronchopneumonia (J18.0)	right
SKO3	female	59	05:05	Cardiogenic shock (R57.0)	left and right
SKO9	female	78	03:45	Heart failure unsp. (I50.9)	left and right
SKO11	male	77	02:55	Cardiac arrest, cause unsp. (I46.9)	left and right
SKO13	female	60	03:25	Respiratory arrest (R09.2)	left and right
SKO18	male	85	02:52	Congestive heart failure (I50.0)	right
SKO19	female	61	02:53	Acute transmural infarction of inferior wall (I21.1)	left and right
SKO24	male	79	02:30	Left ventricular failure (I50.1)	left and right
SKIZ1	male	49	05:02	Respiratory failure unsp. (J96.9)	right
SKIZ3	female	71	04:15	Pulmonary embolism with acute cor pulmonale (I26.0)	right
SKIZ4	male	72	~05:30 (imm.)	Septicaemia unsp. (A41.9)	left and right
SKIZ5	female	61	03:59	Heart failure unsp. (I50.9)	left and right
SKIZ7	male	57	02:21	Cardiac arrest, cause unsp. (I46.9)	left and right
SKIZ8	female	71	03:15	Respiratory arrest (R09.2)	left and right
SKIZ9	male	84	02:47	Respiratory arrest (R09.2)	left and right
SKIZ10	female	67	~03:00	Cardiac arrest, cause unsp. (I46.9)	left and right

Abbreviations: diag.: diagnosis, unsp.: unspecified, imm.: immersion fixation, ~: approximate time, SKO#: control subjects, SKIZ#: schizophrenia subjects.

form of neurofilament M and H, especially in pyramidal cells, as detailed in Introduction section; anti-PV antibodies (Swant, mouse for DAB and rabbit for immunofluorescent staining, both 1:5,000), labeling PV-containing terminals and Betz cells. Between each following steps, the sections were washed 3 times with TBS solution for 10 min.

For DAB-immunohistochemistry, we used biotinylated secondary antibody raised against mouse IgG (Vector, 1:250, 2 h). Then, avidin-biotin horseradish peroxidase complex (ABC, Vector, 1:250) was used for one and a half hours. Preincubation with 0,5-mg/ml DAB solution in TRIS buffer was made for 20′ in dark. For the development, 10 μL 1% H_2O_2 solution was added to the DAB solution. Before dehydration, the sections were incubated in 0.5% OsO_4 in 0.1 M PB for 10′ in dark. After 2 × 5' PB, washing 50% to absolute ethanol ascending alcohol series was applied. Between 50% and 70% ethanol steps, the samples were in 1% uranyl-acetate in 70% ethanol solution for 30 min. After rinsing in 2 × 5 min of acetonitrile, samples were mounted to Durcupan (ACM, Fluka).

Further PV-immunostained sections after development of DAB were mounted to slides through chromium gelatine for Nissl-counterstaining. After 1 night drying, the slides were placed in cuvettes and 3-min-long rehydration steps of xylene, absolute-, 90%-, 70%, and 50% ethanol were processed. After 5 min of 1% cresyl violet incubation, the slices were rinsed in 70% ethanol and fixated with acetic acid containing 70% ethanol. Next, they were rinsed in 90% ethanol followed by 3-min-long dehydration steps with absolute ethanol and xylene. Finally, the slices were covered using DePeX (Serva).

For fluorescent immunohistochemistry, after incubation in primary antibodies (anti-SMI32 [Biolegend, mouse 1:4,000] and anti-PV antibody [Swant, rabbit, 1:5,000]), the samples from both hemispheres of 4 control and 4 schizophrenia subjects were incubated with fluorophore-conjugated secondary antibodies (Alexa594 raised in donkey against rabbit, Alexa488 raised in donkey against mouse, Molecular Probes, 1:500 in TBS) for 3 h in dark. Then, autofluorescence was reduced by pH = 5 3 mmol/l cupric sulphate and 50-mmol/l ammonium acetate dilution (Schnell et al. 1999) with 40-min incubation. After that, the slides were mounted from TBS and covered with antifade medium (Vectashield, Vector).

Electron microscopy

The dehydrated, PV-immunolabeled slices from representative control and schizophrenia samples were used for further preparation to electron microscopy. ROIs from layer 5 of the primary motor cortex were re-embedded and 60-nm ultrathin sections of them were put on single slot copper grids. All ROIs contain at least one Betz cell's soma. We have investigated them with transmission electron microscope (Hitachi TEM 7100). PV-immunolabeled perisomatic terminals around Betz cells and their synaptic profiles were checked.

Collecting data

The determination of BA 4 area was detailed in our previous article (Szocsics et al. 2021). In short, the morphological differences of SMI32-immunopositive cells among BA 3a, −4, and 6 were investigated (Brodmann 1909) and we did not distinguish between BA 4a and 4p areas as Geyer et al. (1996) did. The border of the BA4 is clearly visible by the presence of giant pyramidal cells and the size of the layer 3 pyramidal cells.

All camera lucida drawings were made with a Leitz Dialux 20 microscope. Digital light microphotographs were captured using Nikon Eclipse Ci microscope and NIS Elements BR software.

We sampled 3–6 pieces of 0.5-mm-wide bands of the BA 4 from layer 1 and 5 using camera lucida with 20× objective magnification (Plan, NA = 0.45) from each subject and both hemispheres. The SMI32-immunopositive cell bodies were drawn, and their size was determined with the formula of ellipse: $A = ab\pi/4$, where a and b are the axial and horizontal diameters of the cell body. We counted the number of SMI32-immunpositive cells in layer 3 and 5 and the number was divided by the area of the layer in the band to determine density values (number of cells/mm^2).

Layer 5 of BA4 in SMI32-immunolabeled slices were sampled with 10× objective magnification (Plan, NA = 0.25) microphotographs and the Betz cells' density was calculated by dividing the number of cells with the area of the layer. The images were merged and the layer area was marked with the tools of Photoshop CS6.

The soma area of the giant pyramidal neurons was measured in PV-immunolabeled samples. As we showed earlier, the majority of Betz cells are PV-immunopositive (Szocsics et al. 2021), and 20× objective magnification (Plan, NA = 0.45) camera lucida drawings

of Betz cells were prepared from the whole BA 4 area and soma areas were calculated with the formula of the ellipse as above.

PV-immunostained sections with cresyl violet counterstaining were investigated to determine the Betz cells' PV-content. We made photographs of Betz cells at 40× objective magnification from 2 to 4 sections of each sample searching for all Betz cells in the BA 4 to determine if they show PV-immunopositivity and to count them. The investigator was unaware of which group the samples belonged to. The proportion of PV-immunopositive Betz cells was compared between groups and hemispheres.

Immunofluorescent slices were used in Nikon C2 confocal laser microscope at 60× magnification (oil, Plan Apo, NA = 1.45) to count PV-immunopositive perisomatic terminals of the Betz cells. The images were captured at 1024 × 1024 pixels resolution with NIS Elements AR 4.30 imaging software. The images contain 1 or 2 giant pyramidal neurons at their largest extent. Soma area and perimeters were measured and PV-immunopositive perisomatic terminals were counted if no hiatus between the cell and the terminal was visible. Fiji ImageJ was used for measuring. The images were randomized, and the investigator was not aware of the subjects' group while counting.

All listed data were recorded in Microsoft Excel datasheets. Basic statistics, such as means and standard errors and graphs, were made with the same software. The numbers of cells and terminals included in the study are presented in Table S1.

Animal samples

Eighteen male Sprague–Dawley rats of age 21 days were divided into 3 even groups of 6 animals. They received haloperidol (2 mg/kg, brand name: Haloperidol-Richter, producer: Richter Gedeon), olanzapine (5 mg/kg, brand name: Zyprexa, producer: Lilly), or physiological saline intraperitoneally for 4, 3, and 4 weeks, respectively, to model typical- (haloperidol) and atypical (olanzapine) antipsychotic treatments. The experiment was approved by the Directorate of Food Chain Safety and Animal Health of Pest County Government Office (PEI/001/787–4/2014). The day after the last treatment the animals were perfused through the heart with Zamboni solution with 4% paraformaldehyde and 0,05% of glutaraldehyde in 0.1 M PB, and the brains were removed. Blocks of prefrontal areas were treated and sectioned similarly as detailed above by the human samples. DAB immunochemistry with anti-SMI32 primary antibody was performed on the blocks. The slices were randomized, and the investigator was not aware of which group of animals was examined. Using rat brain atlas (Paxinos and Watson 1998), the primary motor region (M1) was determined. SMI32-positive cells were drawn by camera lucida within 3–8 bands of M1 region per animal, similarly to the human samples above. All data of cell size and number were recorded in Microsoft Excel datasheets. Basic statistics, such as means, standard errors, and graphs, were made by the same software. The numbers of cells included in the study are presented in Table S1.

Statistical analyses

All statistical comparisons were prepared with Tibco Statistica 13.5. The mean soma area and density of SMI32-immunpositive pyramidal and Betz cells were determined for each subject, hemispheres, and layers distinctively. These values were compared using Mann–Whitney U tests. We checked if we can find any difference between layer 3–5, left–right hemispheres, or control and schizophrenia subjects.

In the animal model, hemispheres were not differentiated, and Betz cells cannot be distinguished (Jacobs et al. 2018); therefore, it was not measured distinctively. The haloperidol- and olanzapine-treated animals were compared with the same control group independently.

Furthermore, we compared the proportions of PV-immunopositive Betz cells between subjects and hemispheres. The mean of perisomatic PV-positive terminals contacting Betz cell's somas per 100-μm perimeter was determined and compared between subject groups. Finally, we used the pooled dataset of the terminals of the controls and subjects with schizophrenia. Mann–Whitney U tests were applied for the analyses, except for the investigation of the PV-content of Betz cells, where Student's *t*-tests were applied. Multiple regression analyses were made to determine if any measured features were determined by age or PMI. Graphs were made with Microsoft Excel 2016 or Tibco Statistica 13.5.

Results

PMI and age differences

Detailed data of patients regarding gender, age, and PMI are shown in Table 1. Both groups contain 4 female and 4 male subjects. The mean age of control subjects was 72 ± 10 years, while by patients with schizophrenia: 67 ± 11 years. The mean PMI of control subjects was 3 h33' ± 59, "while of patients with schizophrenia: 3h50"65'. Various causes of death occur in both groups, in majority cardiac and respiratory conditions. The nonparametric comparisons of PMI and age showed no significant difference (Table S2) between subject groups.

SMI32-immunopositive pyramidal cells of layer 3 and 5

In harmony with previous findings, SMI32-immunoreactive cells are present mostly in layer 3 and 5 in the primary motor cortex (Hayes and Lewis 1992), and all Betz cells are strongly labeled (Fig. 1a, d) (Tsang et al. 2000). These were common findings in control and schizophrenia samples in both hemispheres. We measured the density (1/mm^2) and sizes (maximal area—μm^2) of SMI32-immunopositive pyramidal cells of layer 3 and layer 5 in the primary cortex of both hemispheres in 8 control and 8 schizophrenia subjects. The 2 groups were compared with regard to hemispheres as well. Densities of SMI32-positive pyramidal cells did not differ significantly according to the statistical analysis (Fig. 2a–c and e–g; Tables 2 and S2). Statistically significant but minor decline was present in SMI32-positive cell's density of layer 5 when the PMI was higher (Fig. S1).

The mean size of maximal cell areas did not differ between control and schizophrenia groups in both layers and hemispheres (Table S2, not shown in diagram). Afterward, we have investigated the size distribution of pyramidal cell somata in subject groups (Fig. 2d, h). Interestingly, in layer 5 of both hemispheres of schizophrenia subjects, the cells with larger soma area (more than 450 μm^2) were present in smaller proportion, compared with control (Mann–Whitney U = 50.00, N1 = 14, N2 = 14, P = 0.027 two sided, Fig. 2) These cells are larger than 30 μm in longitudinal diameter. Statistically significant but minor increase was present in SMI32-positive cell's size of layer 5 when the PMI was higher (Fig. S1). Statistical analyses are listed in detail in Table S2.

Betz cells

Giant pyramidal cells were investigated as a distinct cell population. They were determined through morphological characteristics, such as large soma size and lipofuscin deposits, conspicuous nucleolus, and circumferential dendrites (Rivara et al. 2003). The density of Betz cells was significantly smaller in the right hemisphere in schizophrenia patients (Mann–Whitney U = 13.00,

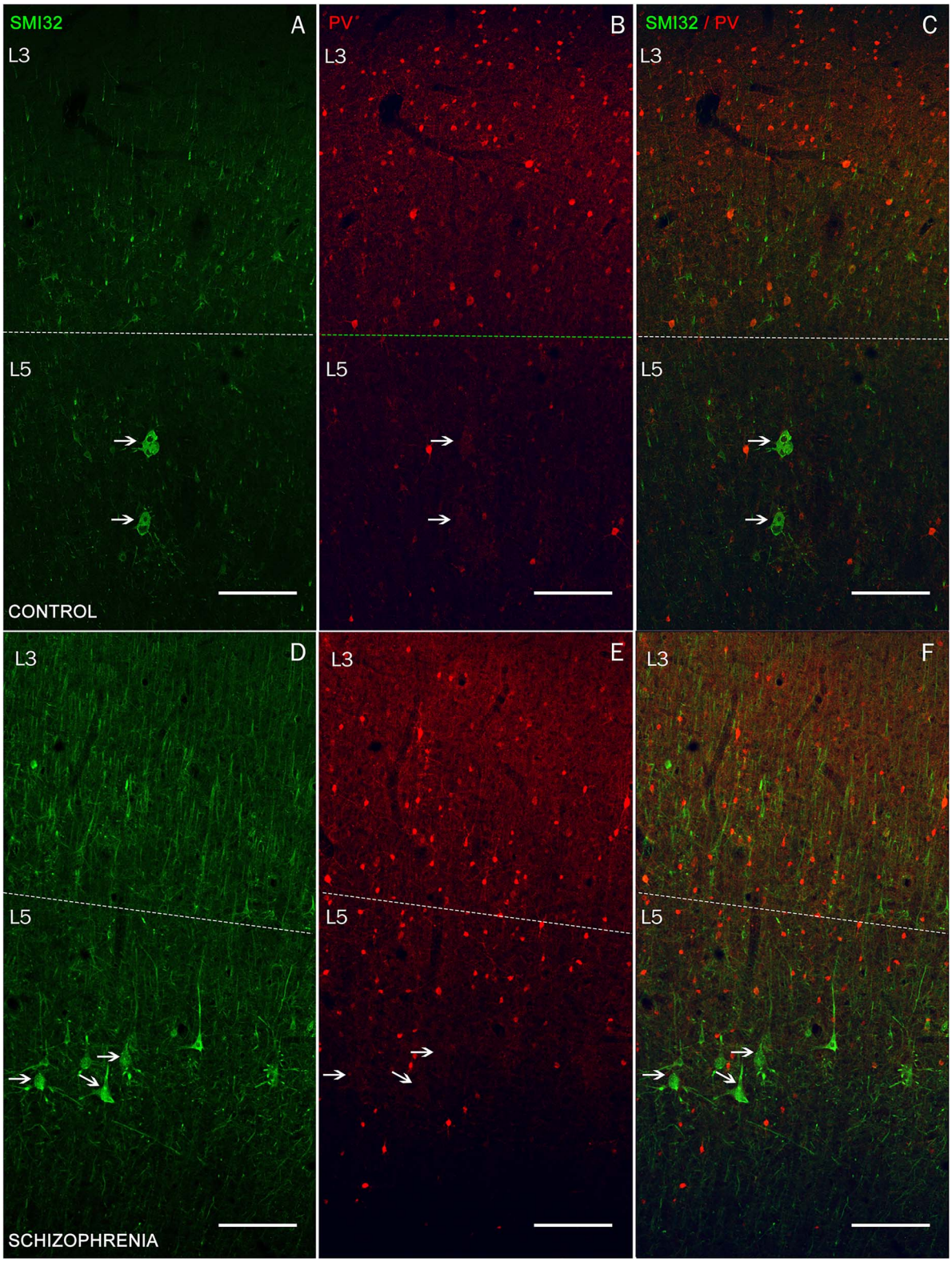

Fig. 1. Low magnitude (4×) confocal microphotographs of the BA 4 area labeled with SMI32 (green) and PV (red). A–C) A control, D–F) a schizophrenia sample. A, D) Only SMI32+ labeling, B, E) only PV labeling, and C, F) both. Dashed lines: borders between layer 3 and 5. Arrows show Betz cells. A high number of layer 3 (L3) and layer 5 (L5) pyramidal cells are labeled by SMI32+ immunostaining in these two layers. Betz cells can be recognized by both immunolabeling (A and B). **Scale**: 250 μm.

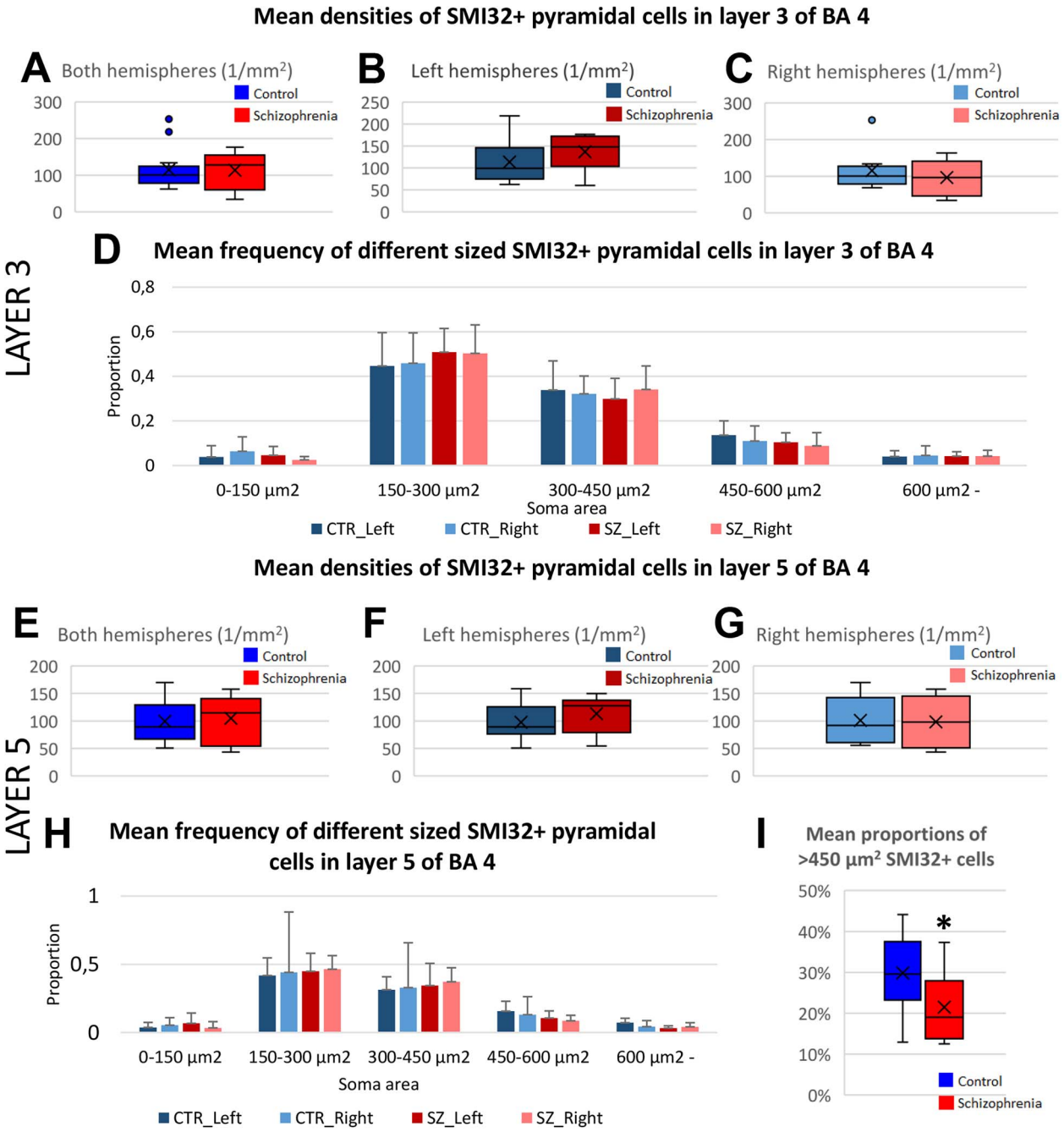

Fig. 2. Graphical representation of the results measuring SMI32+ pyramidal cells in layer 3 (A–D) and 5 (E–I). No significant differences were found in density and mean cell size (Table S2). The diagrams of panels H and I show that cells of layer 5 with larger than 450 μm^2 soma size are proportionately decreased in schizophrenia cases (Mann–Whitney U = 50.00, N1 = 14, N2 = 14, P = 0.027 two sided). Bluish colors: Controls (CTR#), reddish colors: Schizophrenia samples (SZ#). Left hemisphere: #_Left, right hemisphere: #_Right.

N1 = 8, N2 = 8, P = 0.050, two sided). The other comparisons of cell sizes (areas) and densities did not show significant differences among subject groups or hemispheres (Fig. 3, Table S2). Similarly to the other SMI32-immunopositive pyramidal cells, the density of Betz cells showed a minor but significant decrease when the PMI was longer (Fig. S2).

Animal model

Sprague–Dawley rats were treated with saline (control—CON), haloperidol- (HAL), or olanzapine (OLA), 6 animals in each group. No behavioral experiments were carried out on the animals, but the groups were monitored after treatment for 30 min. Major sedation effect was observed after minutes of haloperidol or olanzapine medication.

Camera lucida drawings of the mean soma size and density of SMI-32-immunopositive pyramidal cells of layers 3 and 5 in M1 were measured and compared among the groups. In contrast to human findings, the cell populations of treated animals showed no difference in density, mean cell size, or the proportion of larger size neurons (Fig. 4, Table S3). Interestingly, the density of SMI32-immunopositive cells was higher in layer 5 compared with layer 3 in all groups, while we did not observe similar difference in human primary motor cortices (Table 2).

Table 2. Mean cell density and soma size of SMI32-immunoreactive neurons in human and rat primary motor cortex samples.

Samples			Mean cell density (±S.E. 1/mm^2)		Mean soma size (±S.E. μm^2)	
			Left	Right	Left	Right
Human	**CTR**	**layer 3**	113.47 ± 56.05	115.90 ± 59.17	349.92 ± 54.79	330.83 ± 72.20
		layer 5	97.81 ± 36.04	101.15 ± 42.60	522.83 ± 113.86	465.77 ± 94.44
	SZ	**layer 3**	136.95 ± 42.98	96.84 ± 48.51	329.04 ± 55.77	327.72 ± 39.29
		layer 5	113.41 ± 35.51	98.39 ± 46.27	430.43 ± 137.00	425.88 ± 83.26
Rat	**CON**	**layer 3**	58.89 ± 19.69		134.91 ± 44.31	
		layer 5	113.38 ± 28.48		195.68 ± 53.30	
	HAL	**layer 3**	71.10 ± 13.80		151.37 ± 31.78	
		layer 5	106.46 ± 20.83		235.08 ± 61.69	
	OLA	**layer 3**	88.39 ± 19.39		153.21 ± 20.19	
		layer 5	115.51 ± 21.06		229.89 ± 30.59	

Abbreviations: S.E.: standard error, CTR: control human samples, SZ: schizophrenia samples, CON: saline-treated rat samples, HAL: haloperidol-treated rat samples, OLA: olanzapine-treated rat samples.

PV-content of Betz cells

The proportion of PV-immunopositive Betz cells was measured on DAB-labeled samples with Nissl counterstaining (Fig. 5). No significant difference was found between control and schizophrenia samples (Fig. 5, Table S2). About half of the Betz cells showed PV-immunopositivity in both groups (control samples: left hemispheres: 55.19 ± 11.49%, right hemispheres: 50.83 ± 9.50%; schizophrenia samples: left hemispheres: 56.02 ± 10.90%, right hemispheres: 57.03 ± 11.53%), which was less intense compared with PV-immunopositive interneurons in the most cases (Szocsics et al. 2021) (Figs 1 and 5). Multiple regression analysis showed that the proportion of PV-labeled Betz cells has decreased with age (Fig. 5).

PV-immunopositive perisomatic terminals on Betz cells

Immunofluorescent samples were analyzed by confocal laser scanning microscope (Fig. 6a). PV-immunopositive inputs (mean terminal count per 100 μm cell body perimeter) were decreased on the Betz cells in the right hemispheres of the schizophrenia subjects (Mann–Whitney U = 10320.00, N1 = 149, N2 = 166, P = 0.011. CTR: 5.74 ± 2.22 terminals/100 μm SZ: 5.15 ± 2.01 terminals/100 μm), if the data were pooled (Fig. 6b). Morphological comparison of the left or both hemispheres together showed no significant differences (Table S2). We checked and confirmed that the majority of the PV-immunopositive terminals form synapses on Betz cells both in control and in patients with schizophrenia (Fig. 7).

Discussion

In our study, primary motor cortices of 8 control and 8 schizophrenia subjects were examined by immunohistochemical methods postmortem. Perfusion fixed samples with 2.5–5.5 h PMIs were selected for the study. Whenever possible, both hemispheres of the subjects were included in the investigation. Our results showed that the proportion of large SMI32-immunopositive pyramidal cells was decreased among the total number of pyramidal cells in schizophrenia samples. Similarly, the giant pyramidal cells of the right hemisphere showed a decrease in number, and their perisomatic PV input density (number of terminals per unit perimeter) was dropped, which can indicate a special vulnerability of the Betz cells in the right hemisphere of the schizophrenia patients.

One of the main limitations of our study is the relatively low number of cases examined. Namely, schizophrenia shows high variability genetically (Pardiñas et al. 2018) and in clinical features as well (Tandon et al. 2009; Helldin et al. 2020). By structural magnetic resonance investigations (MRI), 3 distinct biotypes of psychotic disorders are distinguishable in concordance with gray matter reduction (Ivleva et al. 2017), which is not known in samples of this study. Several genetic and environmental factors could play role in the development of schizophrenia (Owen et al. 2016), and 8 (in the immunofluorescent investigation 4) cases are not enough to cover every possibility. Neurological soft signs (Peralta et al. 2010) and other milder motor symptoms (Walther and Strik 2012) did not reach the threshold of clinical significance; therefore, these data are not available for investigation and retrospective data collection was not possible. Thus, in most cases, we only know if patients have ever experienced clinically significant EPSs (Divac et al. 2014) or other motor disturbances during their treatment. EPS occurred in 2 schizophrenia cases, and 2 other patients had catatonic symptoms during their treatment (Table 3). These clinical data showed no correlation with our findings regarding to the density of SMI-32-immunopositive pyramidal neurons or the decrease of perisomatic PV input on Betz cells.

We should add to the limitations that we made some simplifications during the analysis of cell's density and area. For example, these cells were treated as ellipsoids, while the morphology could be more diverse, or that we measured a lower number of sections, than needed for a stereological investigation. The pyramidal cells have a characteristic shape, letting us to consider them as ellipsoid. Furthermore, randomized sampling method and the use of representative sections made it possible to have relevant data during the process.

Another important limitation is that only the PV-immunopositive perisomatic terminals on giant pyramidal cells were examined and we did neither include other pyramidal cells in this investigation nor other subcellular targets of PV-interneurons, such as proximal dendrites or axon initial segment. Therefore, it is not determined at present whether this change is unique to Betz cells or other pyramidal cell populations show similar changes. However, since high number of PV-terminals terminate on the cell body of giant pyramidal cells (Szocsics et al. 2021), the most striking changes may appear on these neurons. Studies of other cortical areas show alterations of PV-containing cells and terminals in schizophrenia (Lewis et al. 2012). Our results supported the presence of similar changes in BA 4 (Fig. 6).

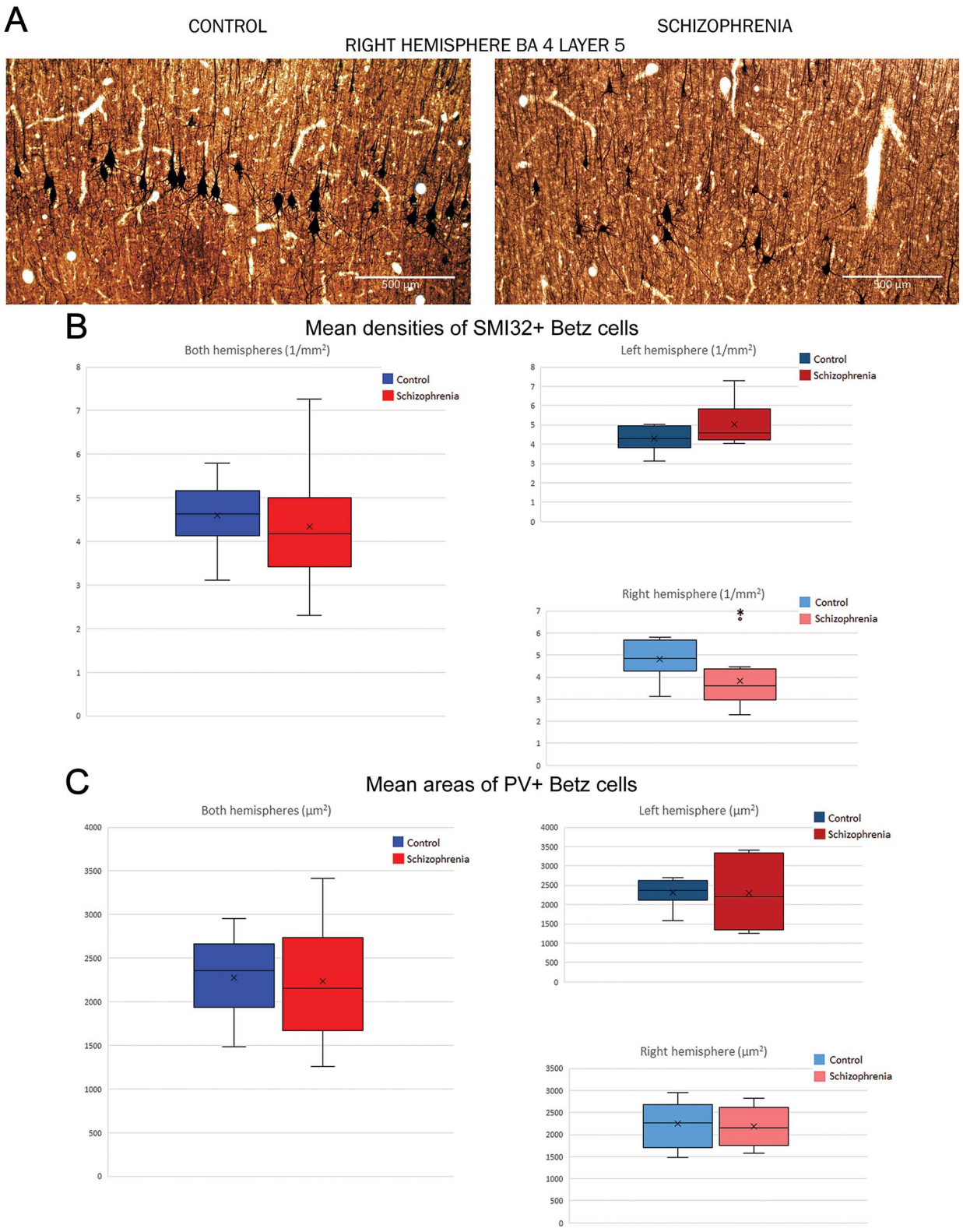

Fig. 3. A) Representative low power images of right hemisphere BA 4 layer 5 s from one control and one schizophrenia sample. As we show in (B), the majority of the cases have decreased density of Betz cells in this area (Mann–Whitney $U = 13.00$, $N1 = 8$, $N2 = 8$, $P = 0.050$, two sided), but not in the left hemisphere. C) Betz cells' area did not differ significantly between control and schizophrenia cases. Shades of blue: Controls, shades of red: Schizophrenia samples.

Primate studies implicate that Betz cells and other cortico-motoneuronal connection establishing BA 4 pyramidal cells play a major role in precision movements (Bennett and Lemon 1996). It was measured earlier that neuronal soma size, axonal diameter, and conduction velocity show correlation in pyramidal tract cells (Sakai and Woody 1988), at least in cats. In addition, BA 4 large pyramidal tract neurons show fast spiking characteristics compared with other pyramidal cells (Vigneswaran et al. 2011).

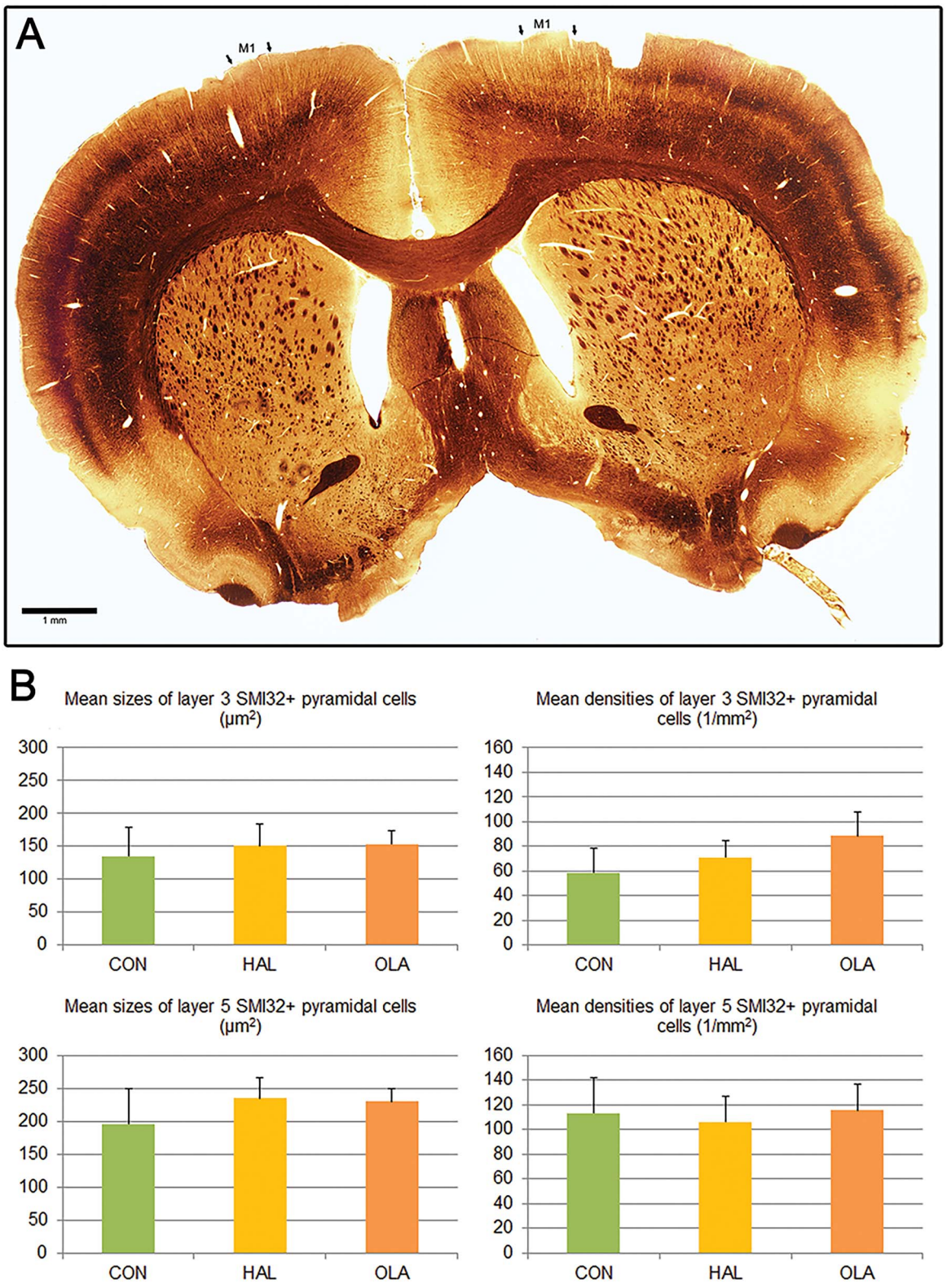

Fig. 4. Animal model of chronic antipsychotic treatment. The picture of (A) shows an SMI32-immunostained rat brain slice, the primary motor areas (M1) are indicated. The diagrams of (B) show that we did not find any change in SMI32-immunopositive pyramidal cell size and density in layer 3 and 5 of M1 among control (CON), haloperidol- (HAL), or olanzapine-treated (OLA) groups (Table S3). Interestingly, the density of SMI32-immunopositive cells was higher in layer 5 compared with layer 3 in all groups, while we did not observe similar difference in human primary motor cortices (Table 2).

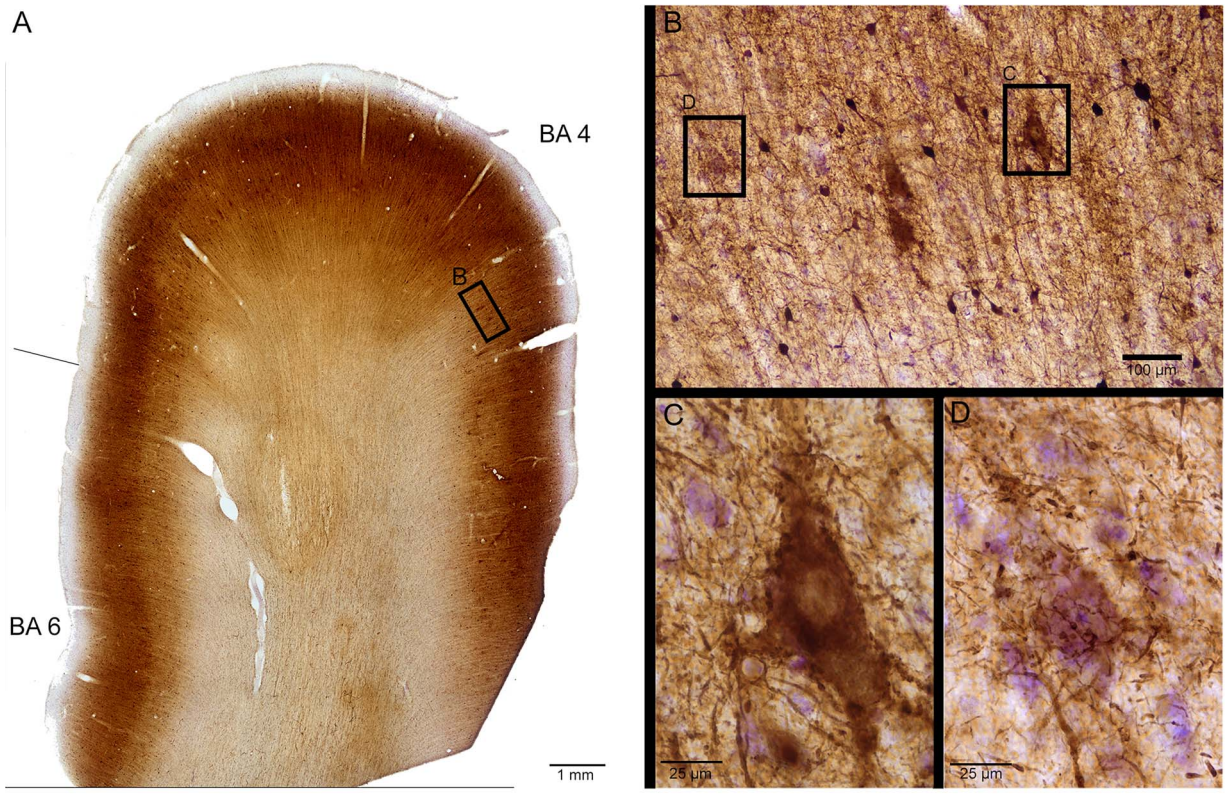

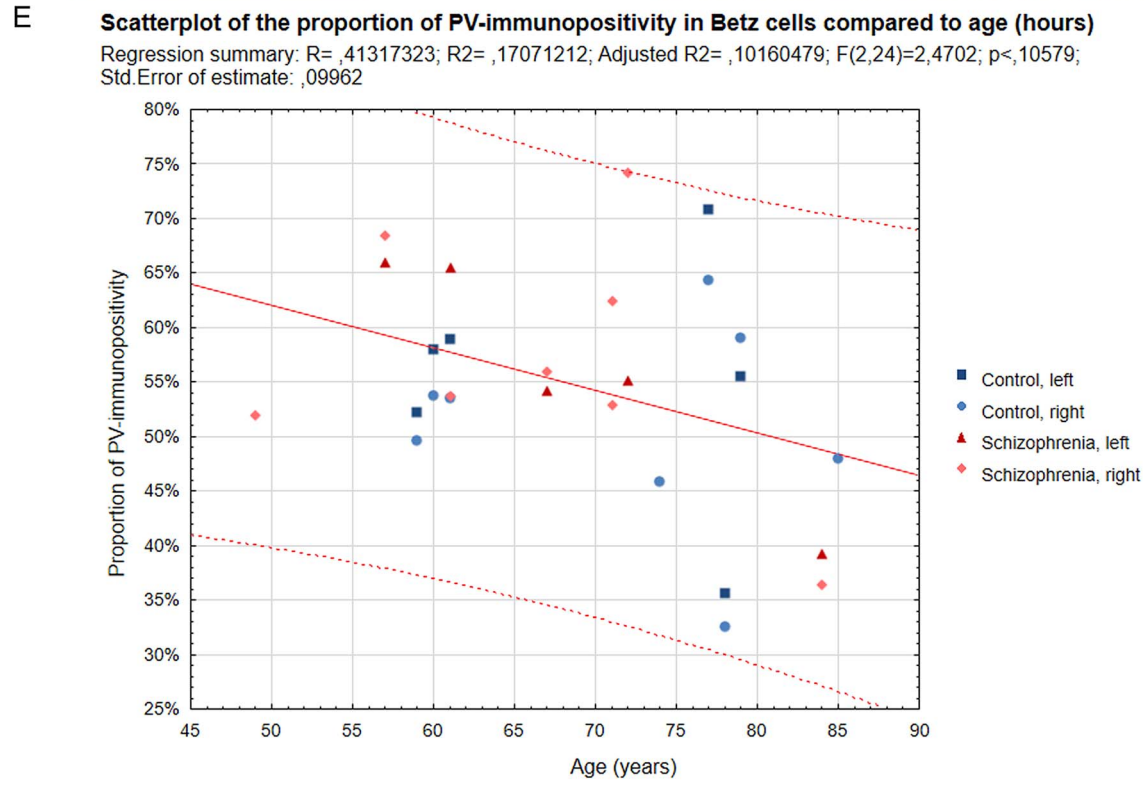

Fig. 5. The proportion of PV-immunopositive Betz cells in control and schizophrenia subjects. A) Low-magnification large image of the BA 4 of a control subject (SKO24 left hemisphere) with PV-immunolabeling counterstained by Cresyl violet. Boxed area B is showed at higher magnification on (B). The boxed areas C and D are presenting one PV-immunopositive and one PV-immunonegative Betz cell on (C) and (D), respectively. (E) Scatterplot and multiple regression analysis of the proportion of PV-immunopositive Betz cells and age. There was no difference between control and schizophrenia subjects in PV-immunopositivity; however, the proportion of labeled cells shows a minor decline with age. Shades of blue: Control-, shades of red: Schizophrenia subjects. Fit line and 0.95 confidence interval are indicated on the scatterplot.

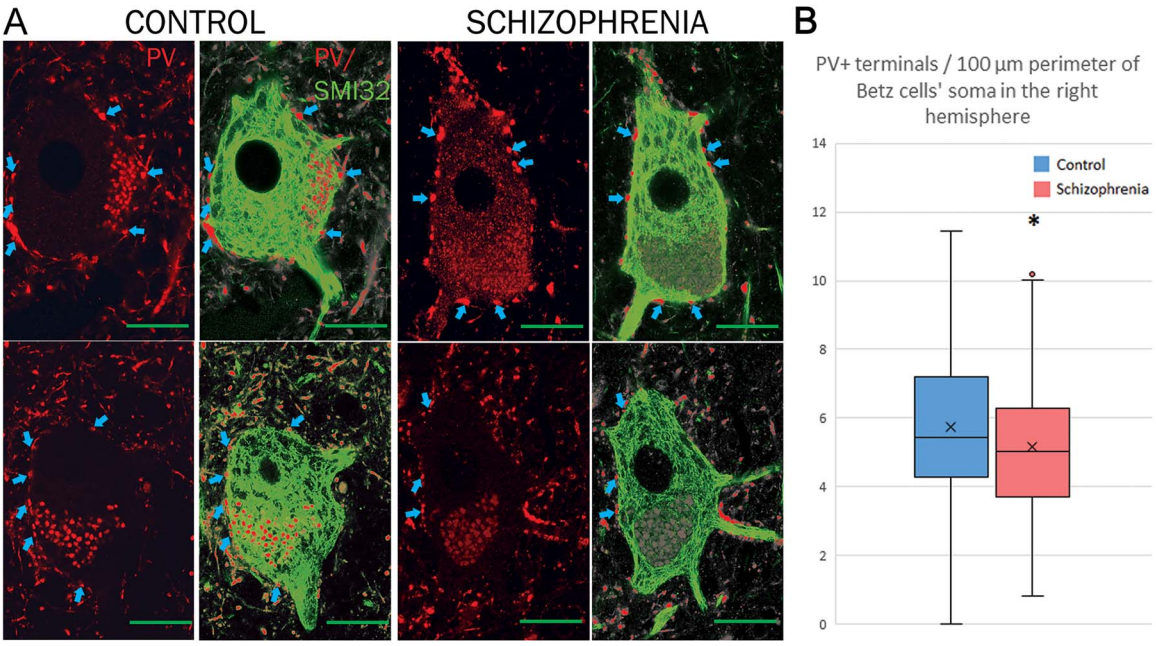

Fig. 6. A) Betz cells from control and schizophrenia samples are shown with high-magnification confocal fluorescent images. Only PV-immunolabeled and with SMI32-staining merged images from each. The Betz cells show different intensities of PV-immunolabeling. Some are very intense, others are PV-negative, or around detection limit. Cyan arrows show PV-immunopositive terminals. **Scale**: 25 μm. B) PV-immunopositive perisomatic terminals of Betz cells were measured and their number determined per 100 μm perimeter on double fluorescent images, as shown in Fig. 5. Statistical analysis revealed that the densities of these terminals are decreased in schizophrenia cases in the right hemisphere (Mann–Whitney U = 10320.00, N1 = 149, N2 = 166, $P = 0.011$).

Table 3. Clinically significant motor disturbances among the examined schizophrenia subjects.

Subject	SKIZ1	SKIZ3	SKIZ4	SKIZ5	SKIZ7	SKIZ8	SKIZ9	SKIZ10
Symptoms	Stupor, EPS	n.a.	n.a.	n.a.	mutism	n.a.	catatonic symptoms	akathisia

Abbreviations: SKIZ#: schizophrenia subject, n.a.: data are not available.

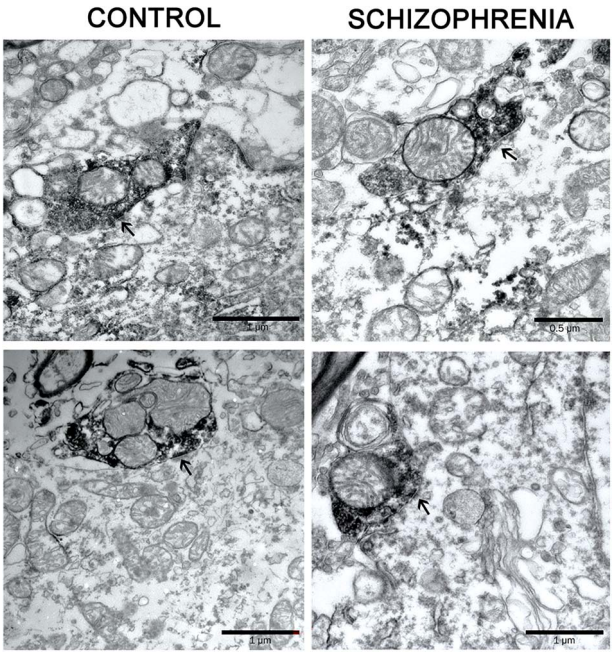

Fig. 7. Electron microscopy pictures of PV-immunopositive terminals and their synapses (arrows) on Betz cells' somata, both in control and schizophrenia subjects.

This might be necessary for the precision required to perform fine movements. The PV content of Betz cells could also be associated with this function. Namely, PV is a calcium buffer protein, which can promote a more rapid mode of action (Arif 2009). Detectable PV-containing Betz cells from control and schizophrenic subjects occurred at a similar proportion (control samples: left hemispheres: 55.19 ± 11.49%, right hemispheres: 50.83 ± 9.50%; schizophrenia samples: left hemispheres: 56.02 ± 10.90%, right hemispheres: 57.03 ± 11.53%). PV-immunoreactivity of Betz cells was in an inverse correlation with the subject's age (Fig. 5). This latter finding might be a neuropathological phenomenon of aging; however, it needs further clarifications. Nevertheless, it was shown earlier that Betz cells are more prone to age-related alterations compared with other pyramidal cells (Scheibel et al. 1977). The decreased number of large pyramidal cells in the right primary motor cortex and decrease in their PV-containing perisomatic inputs may indicate functional disturbances and vulnerability in the right hemisphere. Accordingly, studies showed that the performance of fine motor movements in significant number of patients with schizophrenia is impaired (Carey et al. 2019; Viher et al. 2019). In a significant proportion of patients where mild neurological signs are present (Peralta et al. 2010), some disturbances in brain networks and cells are highly possible. Thus, we believe that our results may help to understand better the etiology of motor impairments.

Many of our results suggest that the right—presumably subdominant—primary motor cortex is more vulnerable in patients with schizophrenia. Some data show that more severe motor disturbances could occur in the left side of the body of later schizophrenia patients (Walker et al. 1994). Other researchers have found either bilateral differences between control and schizophrenia samples (Kreczmanski et al. 2007; Schneiderman et al. 2011) or that the cortical asymmetry between the 2 hemispheres is decreased in patients with schizophrenia (Cullen et al. 2006; Oertel-Knochel et al. 2012). The MRI investigations of white matter tracts show that psychosis patients without catatonia have right lateralized differences compared with healthy controls, while patients with catatonia have opposite differences in the left side especially in corpus callosum (Viher et al. 2020; Wasserthal et al. 2020). The disconnection observed in schizophrenia (Friston et al. 2016) presumably also affects interhemispheric relationship, as previous studies suggest (Hoptman et al. 2012; Mwansisya et al. 2013; von Hohenberg et al. 2014). This may also explain the increase of functional separation between hemispheres, and the reason why the subdominant part might be more involved in some circumstances (Payoux et al. 2004) since the subdominant hemisphere is less connected to other brain regions.

An important question is whether this impairment belongs to the neurodevelopmental nature of schizophrenia (Jaaro-Peled and Sawa 2020), or we observed a secondary, degenerative impairment. Since this study is a postmortem examination, this question cannot be accurately answered by our methods. Developmental studies suggest that motor organization might be affected from an early age (Walker et al. 1994; Sørensen et al. 2010; Dickson et al. 2012), and motor difficulties are present in the clinical high risk for psychosis patients (Dean et al. 2018; Damme et al. 2020), but there is also clinical evidence that patients' motor symptoms deteriorate during the progression of the disease (Chen et al. 2000), which may also be influenced by antipsychotic medication. According to our animal model, SMI32-immunoreactive pyramidal cells are not influenced by high dose treatment of haloperidol or olanzapine; therefore, pharmacological interventions may not play role in the alteration of these pyramidal cells. Thus, we suggest that motor disturbances are most likely the results of neurodevelopmental and degenerative factors simultaneously. Medication itself may not cause changes in the cells of the primary motor cortex. However, the pharmacological treatment in our experimental model was a short period—3–4 weeks, longer exposition to the drugs might also cause alterations in the brain.

In many patients with schizophrenia, the processing of elementary perceptual stimuli is impaired (Butler et al. 2008), whereas a growing number of studies point to the disturbance of motor functions (Walther and Strik 2012). Our research highlights that in addition to brain regions dedicated to higher mental functions, other areas can be also involved in changes caused by schizophrenia and their investigation is essential for understanding the disorder.

Acknowledgments

We would like to thank László Barna, the Nikon Microscopy Center at IEM, Nikon Austria GmbH and Auro-Science Consulting Ltd for kindly providing technical support for fluorescent microscopy. Furthermore, we wish to thank Győző Goda for technical assistance in electron microscopy. The advice and support of Tamás Freund and Cecília Szekeres-Paraczky is also highly appreciated.

CRediT authors statement

Péter Szocsics (Conceptualization, Methodology, Formal analysis, Investigation, Visualization, Project administration, Writing – original draft, Writing – review & editing), Péter Papp (Investigation, Writing – review & editing), László Havas (Resources, Data curation, Writing – review & editing), János Lőke (Resources), Zsófia Maglóczky (Conceptualization, Funding acquisition, Methodology, Project administration, Resources, Supervision, Validation, Writing – original draft, Writing – review & editing).

Supplementary material

Supplementary material is available at *Cerebral Cortex* online.

Funding

National Research, Development and Innovation Office (NKFI, Hungary, K 125436 to ZM); National Brain Research Program (2017-1.2.1-NKP-2017-00002).

Conflict of interest statement: The authors declare that they have no conflicting interest.

Data availability

The datasets generated during and/or analysed during the current study are available from the corresponding author on reasonable request.

Ethical approvals

All procedures were carried out in compliance with the Declaration of Helsinki and approved by the Regional Committee of Science and Research Ethics of Scientific Council of Health (ETT TUKEB 31443/2011/EKU, renewed: ETT TUKEB 15032/2019/EKU).

References

Arif SH. A Ca(2+)-binding protein with numerous roles and uses: parvalbumin in molecular biology and physiology. *BioEssays*. 2009:31(4):410–421. https://doi.org/10.1002/bies.200800170.

Benes FM, Davidson J, Bird ED. Quantitative cytoarchitectural studies of the cerebral cortex of schizophrenics. *Arch Gen Psychiatry*. 1986:43(1):31–35. https://doi.org/10.1001/archpsyc.1986.01800010033004.

Bennett KM, Lemon RN. Corticomotoneuronal contribution to the fractionation of muscle activity during precision grip in the monkey. *J Neurophysiol*. 1996:75(5):1826–1842. https://doi.org/10.1152/jn.1996.75.5.1826.

Betz W. Anatomischer Nachweis zweier Gehirncentra. *Zbl Med Wiss*. 1874:12(578–580):594–599.

Bleuler E. *Dementia praecox or the group of schizophrenias*. New York, NY: International Universities Press; 1950. p. 548.

Boland R, Verduin ML, editors. 5. Schizophrenia Spectrum and other psychotic disorders. In: *Kaplan & Sadock's synopsis of psychiatry*. 12th ed. Philadelphia, PA: Wolters Kluwer; 2021. pp. 337–364.

Brodmann K. *Vergleichende Lokalisationslehre der Grosshirnrinde in ihren Prinzipien dargestellt auf Grund des Zellenbaues*. Leipzig: Barth JA; 1909.

Butler PD, Silverstein SM, Dakin SC. Visual perception and its impairment in schizophrenia. *Biol Psychiatry*. 2008:64(1):40–47. https://doi.org/10.1016/j.biopsych.2008.03.023.

Campbell MJ, Morrison JH. Monoclonal antibody to neurofilament protein (SMI-32) labels a subpopulation of pyramidal neurons in the human and monkey neocortex. *J Comp Neurol*. 1989:282(2): 191–205. https://doi.org/10.1002/cne.902820204.

Carey E, Dooley N, Gillan D, Healy C, Coughlan H, Clarke M, Kelleher I, Cannon M. Fine motor skill and processing speed deficits in young people with psychotic experiences: a longitudinal study. *Schizophr Res*. 2019:204:127–132. https://doi.org/10.1016/j.schres.2018.08.014.

Chen EY, Kwok CL, Au JW, Chen RY, Lau BS. Progressive deterioration of soft neurological signs in chronic schizophrenic patients. *Acta Psychiatr Scand*. 2000:102(5):342–349. https://doi.org/10.1034/j.1600-0447.2000.102005342.x.

Cullen TJ, Walker MA, Eastwood SL, Esiri MM, Harrison PJ, Crow TJ. Anomalies of asymmetry of pyramidal cell density and structure in dorsolateral prefrontal cortex in schizophrenia. *Br J Psychiatry J Ment Sci*. 2006:188(1):26–31. https://doi.org/10.1192/bjp.bp.104.008169.

Damme KSF, Osborne KJ, Gold JM, Mittal VA. Detecting motor slowing in clinical high risk for psychosis in a computerized finger tapping model. *Eur Arch Psychiatry Clin Neurosci*. 2020:270(3):393–397. https://doi.org/10.1007/s00406-019-01059-0.

Dean DJ, Walther S, Bernard JA, Mittal VA. Motor clusters reveal differences in risk for psychosis, cognitive functioning, and thalamocortical connectivity: evidence for vulnerability subtypes. *Clin Psychol Sci*. 2018:6(5):721–734. https://doi.org/10.1177/2167702618773759.

Dickson H, Laurens KR, Cullen AE, Hodgins S. Meta-analyses of cognitive and motor function in youth aged 16 years and younger who subsequently develop schizophrenia. *Psychol Med*. 2012:42(4): 743–755. https://doi.org/10.1017/S0033291711001693.

Divac N, Prostran M, Jakovcevski I, Cerovac N. Second-generation antipsychotics and extrapyramidal adverse effects. *Biomed Res Int*. 2014:2014:656370. https://doi.org/10.1155/2014/656370.

Dum RP, Strick PL. Motor areas in the frontal lobe of the primate. *Physiol Behav*. 2002:77(4):677–682. https://doi.org/10.1016/S0031-9384(02)00929-0.

Filatova S, Koivumaa-Honkanen H, Hirvonen N, Freeman A, Ivandic I, Hurtig T, Khandaker GM, Jones PB, Moilanen K, Miettunen J. Early motor developmental milestones and schizophrenia: a systematic review and meta-analysis. *Schizophr Res*. 2017:188: 13–20. https://doi.org/10.1016/j.schres.2017.01.029.

Friston K, Brown HR, Siemerkus J, Stephan KE. The dysconnection hypothesis (2016). *Schizophr Res*. 2016:176(2):83–94. https://doi.org/10.1016/j.schres.2016.07.014.

Geyer S, Ledberg A, Schleicher A, Kinomura S, Schormann T, Bürgel U, Klingberg T, Larsson J, Zilles K, Roland PE. Two different areas within the primary motor cortex of man. *Nature*. 1996:382(6594): 805–807. https://doi.org/10.1038/382805a0.

Glahn DC, Laird AR, Ellison-Wright I, Thelen SM, Robinson JL, Lancaster JL, Bullmore E, Fox PT. Meta-analysis of gray matter anomalies in schizophrenia: application of anatomic likelihood estimation and network analysis. *Biol Psychiatry*. 2008:64(9):774–781. https://doi.org/10.1016/j.biopsych.2008.03.031.

Glausier JR, Konanur A, Lewis DA. Factors affecting ultrastructural quality in the prefrontal cortex of the postmortem human brain. *J Histochem Cytochem*. 2019:67(3):185–202. https://doi.org/10.1369/0022155418819481.

Groos WP, Ewing LK, Carter CM, Coulter JD. Organization of corticospinal neurons in the cat. *Brain Res*. 1978:143(3):393–419. https://doi.org/10.1016/0006-8993(78)90353-0.

Harrison PJ. The neuropathology of schizophrenia. A critical review of the data and their interpretation. *Brain J Neurol*. 1999:122(Pt 4): 593–624. https://doi.org/10.1093/brain/122.4.593.

Hashimoto T, Bazmi HH, Mirnics K, Wu Q, Sampson AR, Lewis DA. Conserved regional patterns of GABA-related transcript expression in the neocortex of subjects with schizophrenia. *Am J Psychiatry*. 2008:165(4):479–489. https://doi.org/10.1176/appi.ajp.2007.07081223.

Hayes TL, Lewis DA. Nonphosphorylated neurofilament protein and Calbindin immunoreactivity in layer III pyramidal neurons of human neocortex. *Cereb Cortex*. 1992:2(1):56–67. https://doi.org/10.1093/cercor/2.1.56.

Helldin L, Mohn C, Olsson A-K, Hjärthag F. Neurocognitive variability in schizophrenia spectrum disorders: relationship to real-world functioning. *Schizophr Res Cogn*. 2020:20:100172. https://doi.org/10.1016/j.scog.2020.100172.

Hidese S, Ota M, Sasayama D, Matsuo J, Ishida I, Hiraishi M, Teraishi T, Hattori K, Kunugi H. Manual dexterity and brain structure in patients with schizophrenia: a whole-brain magnetic resonance imaging study. *Psychiatry Res Neuroimaging*. 2018:276:9–14. https://doi.org/10.1016/j.pscychresns.2018.04.003.

Hirjak D, Meyer-Lindenberg A, Kubera KM, Thomann PA, Wolf RC. Motor dysfunction as research domain in the period preceding manifest schizophrenia: a systematic review. *Neurosci Biobehav Rev*. 2018:87:87–105. https://doi.org/10.1016/j.neubiorev.2018.01.011.

Hof PR, Nimchinsky EA, Morrison JH. Neurochemical phenotype of corticocortical connections in the macaque monkey: quantitative analysis of a subset of neurofilament protein-immunoreactive projection neurons in frontal, parietal, temporal, and cingulate cortices. *J Comp Neurol*. 1995:362(1):109–133. https://doi.org/10.1002/cne.903620107.

von Hohenberg CC, Pasternak O, Kubicki M, Ballinger T, Vu M-A, Swisher T, Green K, Giwerc M, Dahlben B, Goldstein JM, et al. White matter microstructure in individuals at clinical high risk of psychosis: a whole-brain diffusion tensor imaging study. *Schizophr Bull*. 2014:40(4):895–903. https://doi.org/10.1093/schbul/sbt079.

Hoptman MJ, Zuo X-N, 'Angelo D D, Mauro CJ, Butler PD, Milham MP, Javitt DC. Decreased interhemispheric coordination in schizophrenia: a resting state fMRI study. *Schizophr Res*. 2012:141(1):1–7. https://doi.org/10.1016/j.schres.2012.07.027.

Ivleva EI, Clementz BA, Dutcher AM, Arnold SJM, Jeon-Slaughter H, Aslan S, Witte B, Poudyal G, Lu H, Meda SA, et al. Brain structure biomarkers in the psychosis biotypes: findings from the bipolar-schizophrenia network for intermediate phenotypes. *Biol Psychiatry*. 2017:82(1):26–39. https://doi.org/10.1016/j.biopsych.2016.08.030.

Jaaro-Peled H, Sawa A. Neurodevelopmental factors in schizophrenia. *Psychiatr Clin North Am*. 2020:43(2):263–274. https://doi.org/10.1016/j.psc.2020.02.010.

Jacobs B, Garcia ME, Shea-Shumsky NB, Tennison ME, Schall M, Saviano MS, Tummino TA, Bull AJ, Driscoll LL, Raghanti MA, et al. Comparative morphology of gigantopyramidal neurons in primary motor cortex across mammals. *J Comp Neurol*. 2018:526(3): 496–536. https://doi.org/10.1002/cne.24349.

Kaar SJ, Angelescu I, Marques TR, Howes OD. Pre-frontal parvalbumin interneurons in schizophrenia: a meta-analysis of post-mortem studies. *J Neural Transm (Vienna, Austria: 1996)*. 2019:126(12):1637–1651. https://doi.org/10.1007/s00702-019-02080-2.

Kirkcaldie MTK, Dickson TC, King CE, Grasby D, Riederer BM, Vickers JC. Neurofilament triplet proteins are restricted to a subset of neurons in the rat neocortex. *J Chem Neuroanat*. 2002:24(3):163–171. https://doi.org/10.1016/s0891-0618(02)00043-1.

Kraepelin E. *Dementia praecox and paraphrenia*. Chicago: Chicago Medical Book Co.; 1919. http://archive.org/details/dementiapraecoxp00kraeiala.

Kreczmanski P, Heinsen H, Mantua V, Woltersdorf F, Masson T, Ulfig N, Schmidt-Kastner R, Korr H, Steinbusch HWM, Hof PR, et al. Volume, neuron density and total neuron number in five subcortical regions in schizophrenia. *Brain: a. J Neurol*. 2007:130(Pt 3):678–692. https://doi.org/10.1093/brain/awl386.

Lee VM, Otvos L, Carden MJ, Hollosi M, Dietzschold B, Lazzarini RA. Identification of the major multiphosphorylation site in mammalian neurofilaments. *Proc Natl Acad Sci*. 1988:85(6):1998–2002. https://doi.org/10.1073/pnas.85.6.1998.

Lemon RN. Descending pathways in motor control. *Annu Rev Neurosci*. 2008:31(1):195–218. https://doi.org/10.1146/annurev.neuro.31.060407.125547.

Lewis DA, Curley AA, Glausier JR, Volk DW. Cortical parvalbumin interneurons and cognitive dysfunction in schizophrenia. *Trends Neurosci*. 2012:35(1):57–67. https://doi.org/10.1016/j.tins.2011.10.004.

Lipska BK, Lerman DN, Khaing ZZ, Weickert CS, Weinberger DR. Gene expression in dopamine and GABA systems in an animal model of schizophrenia: effects of antipsychotic drugs. *Eur J Neurosci*. 2003:18(2):391–402.

McGrath J, Saha S, Chant D, Welham J. Schizophrenia: a concise overview of incidence, prevalence, and mortality. *Epidemiol Rev*. 2008:30(1):67–76. https://doi.org/10.1093/epirev/mxn001.

Mwansisya TE, Wang Z, Tao H, Zhang H, Hu A, Guo S, Liu Z. The diminished interhemispheric connectivity correlates with negative symptoms and cognitive impairment in first-episode schizophrenia. *Schizophr Res*. 2013:150(1):144–150. https://doi.org/10.1016/j.schres.2013.07.018.

Oertel-Knochel V, Knochel C, Stablein M, Linden DEJ. Abnormal functional and structural asymmetry as biomarker for schizophrenia. *Curr Top Med Chem*. 2012:12(21):2434–2451. https://doi.org/10.2174/156802612805289926.

Omrani M, Kaufman MT, Hatsopoulos NG, Cheney PD. Perspectives on classical controversies about the motor cortex. *J Neurophysiol*. 2017:118(3):1828–1848. https://doi.org/10.1152/jn.00795.2016.

Owen MJ, Sawa A, Mortensen PB. Schizophrenia. *Lancet*. 2016:388(10039):86–97. https://doi.org/10.1016/S0140-6736(15)01121-6.

Pardiñas AF, Holmans P, Pocklington AJ, Escott-Price V, Ripke S, Carrera N, Legge SE, Bishop S, Cameron D, Hamshere ML, et al. Common schizophrenia alleles are enriched in mutation-intolerant genes and in regions under strong background selection. *Nat Genet*. 2018:50(3):381–389. https://doi.org/10.1038/s41588-018-0059-2.

Paxinos G, Watson C. *The rat brain in stereotaxic coordinates*. 4th ed. San Diego, CA: Academic Press; 1998.

Payoux P, Boulanouar K, Sarramon C, Fabre N, Descombes S, Galitsky M, Thalamas C, Brefel-Courbon C, Sabatini U, Manelfe C, et al. Cortical motor activation in akinetic schizophrenic patients: a pilot functional MRI study. *Mov Disord*. 2004:19(1):83–90. https://doi.org/10.1002/mds.10598.

Penfield W, Boldrey E. Somatic motor and sensory representation in the Cerecral cortex of man as studied by electrical stimulation. *Brain*. 1937:60(4):389–443. https://doi.org/10.1093/brain/60.4.389.

Peralta V, Campos MS, De Jalón EG, Cuesta MJ. Motor behavior abnormalities in drug-naïve patients with schizophrenia spectrum disorders. *Mov Disord*. 2010:25(8):1068–1076. https://doi.org/10.1002/mds.23050.

Rivara C-B, Sherwood CC, Bouras C, Hof PR. Stereologic characterization and spatial distribution patterns of Betz cells in the human primary motor cortex. *Anat Rec A: Discov Mol Cell Evol Biol*. 2003:270A(2):137–151. https://doi.org/10.1002/ar.a.10015.

Sakai H, Woody CD. Relationships between axonal diameter, soma size, and axonal conduction velocity of HRP-filled, pyramidal tract cells of awake cats. *Brain Res*. 1988:460(1):1–7. https://doi.org/10.1016/0006-8993(88)90423-4.

Scheibel ME, Tomiyasu U, Scheibel AB. The aging human betz cell. *Exp Neurol*. 1977:56(3):598–609. https://doi.org/10.1016/0014-4886(77)90323-5.

Schneiderman JS, Hazlett EA, Chu K-W, Zhang J, Goodman CR, Newmark RE, Torosjan Y, Canfield EL, Entis J, Mitropoulou V, et al. Brodmann area analysis of white matter anisotropy and age in schizophrenia. *Schizophr Res*. 2011:130(1–3):57–67. https://doi.org/10.1016/j.schres.2011.04.027.

Schnell SA, Staines WA, Wessendorf MW. Reduction of lipofuscin-like autofluorescence in fluorescently labeled tissue. *J Histochem Cytochem*. 1999:47(6):719–730. https://doi.org/10.1177/002215549904700601.

Sørensen HJ, Mortensen EL, Schiffman J, Reinisch JM, Maeda J, Mednick SA. Early developmental milestones and risk of schizophrenia: a 45-year follow-up of the Copenhagen perinatal cohort. *Schizophr Res*. 2010:118(1–3):41–47. https://doi.org/10.1016/j.schres.2010.01.029.

Szocsics P, Papp P, Havas L, Watanabe M, Maglóczky Z. Perisomatic innervation and neurochemical features of giant pyramidal neurons in both hemispheres of the human primary motor cortex. *Brain Struct Funct*. 2021:226(1):281–296. https://doi.org/10.1007/s00429-020-02182-8.

Tandon R, Nasrallah HA, Keshavan MS. Schizophrenia, "just the facts" 4. Clinical features and conceptualization. *Schizophr Res*. 2009:110(1):1–23. https://doi.org/10.1016/j.schres.2009.03.005.

Tsang YM, Chiong F, Kuznetsov D, Kasarskis E, Geula C. Motor neurons are rich in non-phosphorylated neurofilaments: cross-species comparison and alterations in ALS. *Brain Res*. 2000:861(1):45–58. https://doi.org/10.1016/S0006-8993(00)01954-5.

Vigneswaran G, Kraskov A, Lemon RN. Large identified pyramidal cells in macaque motor and premotor cortex exhibit 'thin spikes': implications for cell type classification. *J Neurosci*. 2011:31(40):14235–14242. https://doi.org/10.1523/jneurosci.3142-11.2011.

Viher PV, Docx L, Van Hecke W, Parizel PM, Sabbe B, Federspiel A, Walther S, Morrens M. Aberrant fronto-striatal connectivity and fine motor function in schizophrenia. *Psychiatry Res Neuroimaging*. 2019:288:44–50. https://doi.org/10.1016/j.pscychresns.2019.04.010.

Viher PV, Stegmayer K, Federspiel A, Bohlhalter S, Wiest R, Walther S. Altered diffusion in motor white matter tracts in psychosis patients with catatonia. *Schizophr Res*. 2020:220:210–217. https://doi.org/10.1016/j.schres.2020.03.017.

Walker EF, Savoie T, Davis D. Neuromotor precursors of schizophrenia. *Schizophr Bull*. 1994:20(3):441–451. https://doi.org/10.1093/schbul/20.3.441.

Walther S. Psychomotor symptoms of schizophrenia map on the cerebral motor circuit. *Psychiatry Res*. 2015:233(3):293–298. https://doi.org/10.1016/j.pscychresns.2015.06.010.

Walther S, Strik W. Motor symptoms and schizophrenia. *Neuropsychobiology*. 2012:66(2):77–92. https://doi.org/10.1159/000339456.

Ward KM, Citrome L. Antipsychotic-related movement disorders: drug-induced parkinsonism vs. tardive dyskinesia-key differences in pathophysiology and clinical management. *Neurol Ther*. 2018:7(2):233–248. https://doi.org/10.1007/s40120-018-0105-0.

Wasserthal J, Maier-Hein KH, Neher PF, Northoff G, Kubera KM, Fritze S, Harneit A, Geiger LS, Tost H, Wolf RC, et al. Multiparametric mapping of white matter microstructure in catatonia. *Neuropsychopharmacology*. 2020:45(10):1750–1757. https://doi.org/10.1038/s41386-020-0691-2.